

Cellular Aluminum Particle-Air Detonation Based on Realistic Heat Capacity Model

Xiang GaoXiang, Yang Pengfei, Teng HongHui & Jiang ZongLin

To cite this article: Xiang GaoXiang, Yang Pengfei, Teng HongHui & Jiang ZongLin (2019): Cellular Aluminum Particle-Air Detonation Based on Realistic Heat Capacity Model, Combustion Science and Technology, DOI: [10.1080/00102202.2019.1632298](https://doi.org/10.1080/00102202.2019.1632298)

To link to this article: <https://doi.org/10.1080/00102202.2019.1632298>



Published online: 20 Jun 2019.



Submit your article to this journal [↗](#)



Article views: 14



View Crossmark data [↗](#)



Cellular Aluminum Particle-Air Detonation Based on Realistic Heat Capacity Model

Xiang GaoXiang^{a,b}, Yang Pengfei^b, Teng HongHui^{b,c}, and Jiang ZongLin^b

^aSchool of Mechanics, Civil Engineering & Architecture, Northwestern Polytechnical University, Xi'an, China;

^bState Key Laboratory of High Temperature Gas Dynamics, Institute of Mechanics, Chinese Academy of Sciences, Beijing, China; ^cSchool of Aerospace Engineering, Beijing Institute of Technology, Beijing, China

ABSTRACT

Modeling aluminum (Al) particle-air detonation is extremely difficult because the combustion is shock-induced, and there are multi-phase heat release and transfer in supersonic flows. Existing models typically use simplified combustion to reproduce the detonation velocity, which introduces many unresolved problems. The hybrid combustion model, coupling both the diffused- and kinetics-controlled combustion, is proposed recently, and then improved to include the effects of realistic heat capacities dependent on the particle temperature. In the present study, 2D cellular Al particle-air detonations are simulated with the realistic heat capacity model and its effects on the detonation featured parameters, such as the detonation velocity and cell width, are analyzed. Numerical results show that cell width increases as particle diameter increases, similarly to the trend observed with the original model, but the cell width is underestimated without using the realistic heat capacities. Further analysis is performed by averaging the 2D cellular detonations to quasi-1D, demonstrating that the length scale of quasi-1D detonation is larger than that of truly 1D model, similar to gaseous detonations.

ARTICLE HISTORY

Received 8 July 2016

Revised 12 May 2019



Accepted 12 June 2019

KEYWORDS

Al particle; cellular detonation; heat capacity; hybrid model

Aluminum (Al) particle-air detonations have many engineering applications, from catastrophic accident prevention to rocket propellant combustion (Bartlett, Ong, Fassell et al. 1963; Eckhoff 1993; Melcher, Krier, Burton 2002). The Al-air mixture detonation propagates similar to a gaseous detonation: its post-shock wave combustion produces intensive heat release followed by a sustained, strong leading shock. The Al particle is generally thought to vaporize first, however, which makes the combustion diffusion-controlled – this manner of combustion is characteristic of liquid fuel detonations, whereas gaseous fuel detonation is kinetics-controlled (Glassman, Yetter, Glumac 2014). Al-air detonation has several unique features, for example, Al particles are covered by an aluminum oxide (Al_2O_3) shell affecting detonation ignition by generating solid combustion product Al_2O_3 . These multi-phase interactions make Al combustion very complicated, resulting in many unresolved problems (Dreizin 2000; Zhang 2012).

The chemical reaction time and length scales are much longer for heterogeneous post-shock combustion than those for homogeneous combustion. It is very difficult to carry out dusty detonation experiments, so there have been relatively few Al-air detonation experiments reported in the literature (A J and Selman 1982; Borisov, Khasainov, Saneev et al.

CONTACT Teng HongHui  hhteng@bit.edu.cn  State Key Laboratory of High Temperature Gas Dynamics, Institute of Mechanics, Chinese Academy of Sciences, Beijing 100190, China

© 2019 Taylor & Francis Group, LLC

1991; Liu, Li, Bai 2009; Zhang, Gerrard, Ripley 2009; Zhang, Grönig, Van de 2001). Based on these limited experimental results, however, theoretical and numerical models have been developed to study Al dust detonation. The earliest two-phase model of the considered problem was proposed by Borisov et al. (Borisov, Khasainov, Saneev et al. 1991). Fedorov et al. (Fedorov and Fomin 1999; Fedorov, Fomin, Khmel' 2009; Fedorov, Khmel, Kratova 2008, 2010) developed a non-equilibrium model to calculate detonation parameters as well as both ideal and cellular detonation diffraction to reveal the special characteristics of dusty detonation. Papalexandris (Papalexandris 2004a, 2004b, 2005; Varsakelis and Papalexandris 2011) developed a two-phase model by applying the classical theory of irreversible processes, and examined the structure and stability of detonations in mixtures of gases and solid particles that were either combustible or inert. Benkiewicz et al. (Benkiewicz and Hayashi 2006, 2003) simulated cellular structures of Al-oxygen detonation to examine the influence of particle diameter. Veyssiere et al. (Veyssiere, Khasainov, Briand 2008) studied Al-air and Al-oxygen detonation initiations and found that the critical initiation energy is correlated with the cellular width. All these models are all diffusion-controlled and thus suitable for mild combustion of large particles (Brooks and Beckstead 1995). Recent experiments (Bazyn, Krier, Glumac 2006; Lynch, Fiore, Krier et al. 2010; Lynch, Krier, Glumac 2009; Tanguay, Goroshin, Higgins et al. 2009) have demonstrated that the combustion of particles with diameters below 10 μm is dependent on pressure, i.e., features kinetics-controlled combustion. Zhang et al. (Zhang, Gerrard, Ripley 2009) proposed a hybrid model for simulating this manner of detonation based on a combination of diffusion-controlled and kinetics-controlled combustions, and Briand et al. (Briand, Veyssiere, Khasainov 2010) used the hybrid model for cellular detonation simulations, then compared the results with those from the classic diffusion model.

The hybrid model is one important step toward a comprehensive understanding of Al particle-air detonations, but its accuracy remains insufficient. In this study, we improved the hybrid combustion model with realistic heat capacities that vary with the particle temperature as opposed to the models described above with constant heat capacities. Numerical results (Teng and Jiang 2013) based on 1D simulations showed that using constant heat capacities causes the interior combustion characteristic lengths to be underestimated. In gaseous detonations, interior combustion length is related to cell width, which is the most important dynamic parameter; therefore, the effects of realistic heat capacities on 2D cellular detonations are crucial.

Section 2 introduces the numerical methods we used as well as our main assumption. Section 3 discusses our analysis of the numerical results, and concluding remarks are provided in Section 4.

Governing equations

Because Al density is 3-orders higher than gas density, the volume fraction of the particle is not considered. Furthermore, the particle-particle interactions and viscous terms are also neglected according to previous research. The governing equations of gas mixtures can be written as follows:

$$\frac{\partial U_g}{\partial t} + \frac{\partial E_g}{\partial x} + \frac{\partial F_g}{\partial y} = S_g + H_g$$

The multi-fluid method was used here to model the motion of particles. Its governing equations can be written as:

$$\frac{\partial U_p}{\partial t} + \frac{\partial E_p}{\partial x} + \frac{\partial F_p}{\partial y} = S_p + H_p$$

where S_g and S_p are the source terms derived from chemical reactions for the gas and particle, respectively; H_g and H_p are the source terms derived from gas-particle interactions for the gas and particle, respectively.

To complete these equations, the source terms need to be modeled. The mass exchange was modeled here in the source term S , as discussed below. In the source term H , there are two key parameters – the multi-phase interaction force f , and the convective heat exchange Q_d . The force which dominates the momentum exchange can be written as:

$$\vec{f} = C_d(n_{Al}d_{p,Al}^2 + n_{Al2O3}d_{p,Al2O3}^2)\frac{\pi}{4}\rho(\vec{u} - \vec{u}_p)|\vec{u} - \vec{u}_p|/2$$

and the drag coefficient C_d calculated by:

$$C_d = \frac{24}{Re_s} \left(1 + \frac{1}{6} Re_s^{2/3} \right)$$

where n is the number of particles for each component and d_p is individual particle diameter. The heat exchange term induced by convection Q_d can be written as:

$$Q_d = (n_{Al}d_{p,Al} + n_{Al2O3}d_{p,Al2O3})\pi Nu\lambda(T - T_p)$$

with

$$Nu = 2.0 + 0.459 Re_s^{0.55} Pr^{0.33}$$

$$Re_s = \frac{\rho|\vec{u} - \vec{u}_p|}{\mu}(d_{p,Al} + d_{p,Al2O3})$$

For simplicity, other typical terms (which can be found easily in the literature) are not listed here (Briand, Veyssiere, Khasainov 2010; Teng and Jiang 2013; Zhang, Gerrard, Ripley 2009).

Combustion model and numerical methods

The chemical reaction model for combustions is one of the most important components in detonation simulations. Zhang et al. (Zhang, Gerrard, Ripley 2009) proposed a hybrid model which integrates both diffusion-controlled and kinetics-controlled combustion, and the Al reaction rate in this model is defined as

$$J_{Al} = -n_{Al}\pi d_{p,Al}^2 k_1 = -n_{Al}\pi d_{p,Al}^2 \frac{\nu_{Al} W_{Al}}{\nu_{oxi} W_{oxi}} k$$

with

$$k = k_d(C_{oxi} - C_{oxi,0}), k = k_s C_{oxi,0}$$

where k_1 and k are the Al and oxidizing consumption rate, and k_d and k_s are the diffusion and kinetic reaction rate. ν , W , C_{oxi} , $C_{oxi,0}$ denote the molecular weight, stoichiometric coefficient, oxidizing gas mole concentration, and its particle surface value, respectively. From the above equations, one may get

$$k = \frac{k_d k_s}{k_d + k_s} C_{oxi}$$

For the diffusion-controlled combustion, the reaction rate k_d is

$$k_d = \frac{\nu_{oxi} W_{oxi}}{\nu_{Al} W_{Al}} \frac{\rho_{p,Al} d_{p,Al}}{2 C_{total} K d_{p0,Al}^2} \left(1 + 0.276 \text{Re}_s^{1/2} \text{Pr}^{1/3}\right)$$

For the kinetics-controlled combustion, the reaction rate k_s is

$$k_s = k_0 e^{-E/RT_s}$$

where C_{total} is the total mole concentration, $d_{p0,Al}$ is the initial diameter of the particle, $T_s = (T + T_p)/2$ is the particle surface temperature. K and k_0 are chemical reaction constants. Following previous studies (Bazyn, Krier, Glumac 2006; Benkiewicz and Hayashi 2006, 2003; Briand, Veyssiere, Khasainov 2010; Brooks and Beckstead 1995; Fedorov and Fomin 1999; Fedorov, Fomin, Khmel' 2009; Fedorov, Khmel, Kratova 2008, 2010; Lynch, Fiore, Krier et al. 2010; Lynch, Krier, Glumac 2009; Papalexandris 2004a, 2004b, 2005; Tanguay, Goroshin, Higgins et al. 2009; Varsakelis and Papalexandris 2011; Veyssiere, Khasainov, Briand 2008; Zhang, Gerrard, Ripley 2009), the constants used in the chemical model are $K = 4 \times 10^6 \text{s/m}^2$, $k_0 = 1.2 \times 10^3 \text{kg.m/mol.s}$, and $E = 71.7 \text{kJ/mol}$.

The idea of combining two different reaction models derives from the fact that the diffusion reaction rate is much higher than the kinetic reaction rate in the case of relatively low temperature, e.g. Al melting point 933 K, while the latter is much higher than the former in the case of relatively high temperature, e.g. Al boiling point 2792 K. Generally, the diffusion-controlled reaction rate varies with particle diameter but is independent on the temperature; conversely, the kinetics-controlled reaction rate varies with temperature but is independent on the particle diameter. Hence, the reaction rate predicted by the hybrid model is dominated by the kinetics-controlled rate at low temperature and by the diffusion-controlled reaction at high temperature. It is worth noting that this hybrid model is still an empirical model without knowledge of detailed reaction mechanisms. The ignition and heat release of Al particle is very complicated and sensitive to several parameters, such as the diameter, the heating rate. More work on the Al combustion needs to be done and will play the important role in improving the combustion model.

Besides implementing the detailed chemical reaction mechanisms, the improvement of the combustion model (Zhang, Gerrard, Ripley 2009) can also be achieved by considering the realistic heat capacities depending on the particle temperature. In gaseous detonation studies, the detailed chemical reaction model with realistic gas species properties has been used for years (Oran, Weber, Stefaniw et al. 1998; Tsuboi, Eto, Hayashi 2007), but the

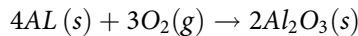
simplified models of Al combustion usually use the constant heat capacity for solid particles, inducing several problems and degenerating the model accuracy. The heat capacity plays the important role in the energy conservation, and may impacts the energy exchange significantly. For example, the heat capacity of Al is 24.2 J/mol·K at 300 K, but 32.3 J/mol·K at 900 K; the heat capacity of an Al_2O_3 particle is 79.3 J/mol·K at 300 K, while 192.5 J/mol·K for liquid Al_2O_3 above 2327 K (Linstrom 2001). The heat capacity of the solid particle is associated with the particle internal energy and the particle temperature, which play an important role in the energy equations and the source terms. For a constant heat capacity, the temperature can be written as

$$T_p = \begin{cases} \frac{e_p/c_{pv}}{T_{p,m}} & e_p \leq c_{pv}T_{p,m} \\ (e_p - L_m)/c_{pv} & \text{for } c_{pv}T_{p,m} < e_p \leq c_{pv}T_{p,m} + L_m \\ \frac{T_{p,b}}{c_{pv}T_{p,b} + L_m} & c_{pv}T_{p,m} + L_m < e_p \leq c_{pv}T_{p,b} + L_m \\ (e_p - L_m - L_b)/c_{pv} & c_{pv}T_{p,b} + L_m < e_p \leq c_{pv}T_{p,b} + L_m + L_b \\ & e_p > c_{pv}T_{p,b} + L_m + L_b \end{cases}$$

where $L_m = 10.7$ KJ/mol denotes the melting latent heat, $L_b = 290$ KJ/mol denotes the evaporation latent heat, c_{pv} is the heat capacity, $T_{p,m}$ is Al melting temperature, and $T_{p,b}$ is the evaporation temperature. To improve the hybrid model, the original constant heat capacity was replaced by an average heat capacity $\bar{c}_p(T_p)$ given by:

$$\bar{c}_p = \int_{T_0}^{T_p} c_{pv}(T) dT / (T_p - T_0)$$

where T_0 is the temperature at the front of the detonation wave and the initial temperature of the fresh medium. In numerical procedures, there are two steps concerning the realistic heat capacities. The first one is to calculate internal energy from the temperature and it could be done by combing above two equations easily. However, here we have used the other one, with temperature calculated from the internal energy. This technique is complicated because the relation between the temperature and internal energy is not linear. The iterative process is necessary to calculate the temperature. To improve the algorithm efficiency, we first calculate the internal energy and generate one list as a function of the given temperature and particle fraction. Then, the temperature calculation is simplified into a list searching process for a given internal energy, which has higher efficiency than the iterative process and does not loss the accuracy. Numerical tests demonstrated that the accuracy can be guaranteed if the temperature interval small enough, which is set to be 5 K in this study. The chemical reaction was simplified as follows:



where the heat release of Al combustion is 838 kJ/mol and Pr number is 0.72. Gas properties were considered to change with temperature (McBride, Zehe, Gordon 2002), but chemical reactions and gas dissociations were neglected. The shock-capturing method is the Dispersion-Controlled Dissipation scheme (Zonglin 2004), a type of TVD scheme that is popular among researchers in this field (Hu, Dou, Khoo 2011; Hu et al. 2015; Teng and Jiang 2013).

Numerical results and discussion

The initial pressure was 2.5 atm and the temperature is 300 K, with Al-particle average density of 1250 g/m³ and without $Al_2O_3(s)$ initially. Gaseous $O_2(g)$ and $N_2(g)$ were in mole concentration of 1:4, while $Al(s)$ and $Al_2O_3(s)$ were used as solid particles. In some models, the $Al(g)$ vapor is included in model if the temperature is above the Al boiling point and the Al_2O_3 could be treated as the gaseous species $Al_2O_3(g)$. Because there are some uncertainties on multi-phase processes, they are not included except the gas-particle force and heat conduction. Following our previous study (Teng and Jiang 2013), the mesh scale is chosen to be 0.5 mm. Resolution experiments with an additional mesh size 2 mm, 1 mm, and 0.2 mm have been performed, and mesh size 0.5 mm is found to be enough. In this study, numerical results are also verified by double the grid resolution.

The high pressure and temperature region is typically used to initiate the detonation. The ignition pressure is 29.05 times the fresh mixture pressure, i.e. 72.625 atm, and the temperature is 1748K, corresponding to the von-Neumann shocked state of the CJ detonation (Zhang, Gerrard, Ripley 2009). In this study, the 2D ignition region locates between the end wall $x = 0$ m and 0.02 m, with the same pressure and temperature as those in a 1D scenario. To form the cellular structure quickly, four 0.05m-height sub-regions with the same parameters as the pre-detonation mixtures are placed in the ignition region, as illustrated in Figure 1. It is worth noting that there are many options for ignition scenario, and we did test several of them. Theoretically, these scenarios would not influence the final cellular structures. It is important to keep the initiation energy large enough to initiate the detonation while not so large that the detonation remains over-driven at the end of the tube; accordingly, the cell width reaches a stable value.

The detonation with initial particle diameter $D_p = 2.0 \mu\text{m}$ was simulated as shown in Figure 2. Numerical results showed that four pairs of transverse waves formed due to the disturbance in the initiation region. However, this structure is unstable and evolves into more weak transverse waves as the detonation propagates downstream. Only very weak but fine transverse waves are observable soon, and this type of detonation structure forms at about $x = 0.5$ m. Until the detonation reaches the downstream boundary, this structure keeps the same so the detonation with weakly disturbed planar leading shock is the final steady state.

The detonation with initial particle diameter $D_p = 3.0 \mu\text{m}$ is shown in Figure 3. Similar to the case described above, four pairs of transverse waves are observed initially due to the initiation. Subsequently, the transverse waves split and generated a greater number of weaker transverse waves in the propagation. Due to the different

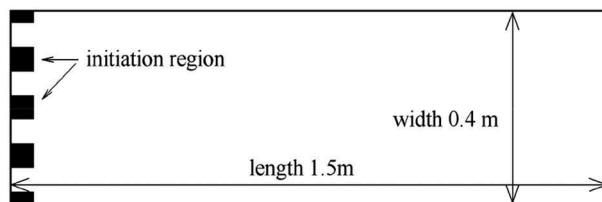


Figure 1. Computation sketch of Al detonation simulation.

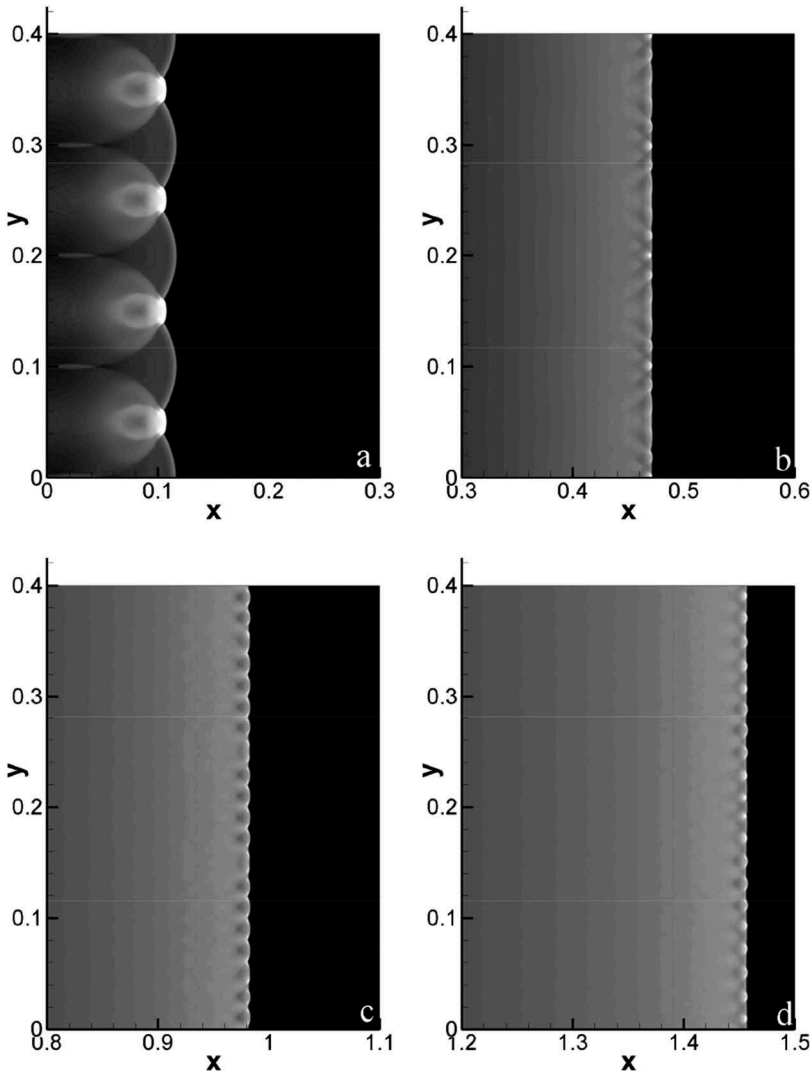


Figure 2. Pressure of cellular detonations based on realistic heat capacity model, $D_p = 2.0 \mu\text{m}$.

particle diameter, we find out that eight pairs of transverse waves formed when the detonation reaches about $x = 0.5$ m. Subsequent simulation up to about $x = 1.5$ m shows that the number of detonation cells remains constant, so the detonation and corresponding

the cellular structure became quasi-steady.

The detonation with initial particle diameter $D_p = 4.0 \mu\text{m}$ is shown in [Figure 4](#). The ignition zone generates four pairs of transverse waves first, similar to the two cases described above. However, the transverse waves don't disappear nor increase in number throughout the entire propagation process. Hence, cellular detonation structure becomes quasi-steady, with four pairs of transverse waves. Taken together, these results show that particle diameter influences cell width, and that cell width increases as diameter increases.

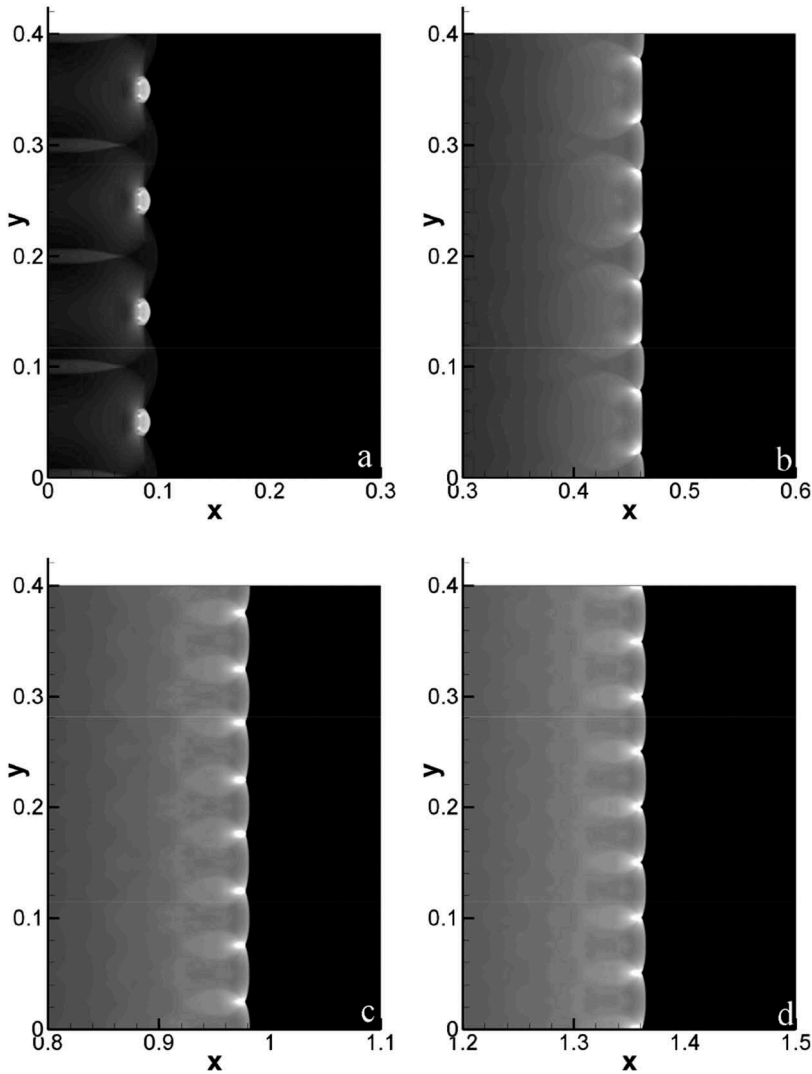


Figure 3. Pressure of cellular detonations based on realistic heat capacity model, $D_p = 3.0 \mu\text{m}$.

The relation between the particle diameter and cell width has been studied before based on the constant heat capacity model (Benkiewicz and Hayashi 2003; Briand, Veyssiere, Khasainov 2010). Similar to these studies, our results based on the realistic heat capacity model also show that the cell width increases with particle diameter. To compare the results from different models and then elucidate the effects of realistic heat capacities, three cases with the constant heat capacity model are simulated with all other parameters kept constant. In the case of $D_p = 2.0 \mu\text{m}$, the detonation wave was a weakly-disturbed planar leading shock, without obvious difference from those shown in Figure 2. However, different transverse waves numbers are observed in the two other cases, as shown in Figure 5. To count the transverse waves clearly, the black line in the heat release region, denotes certain density contours, is also plotted. There are 12 pairs of transverse waves in the case of $D_p = 3.0 \mu\text{m}$, and eight pairs of transverse waves in the case of $D_p = 4.0 \mu\text{m}$. In both cases, the number of

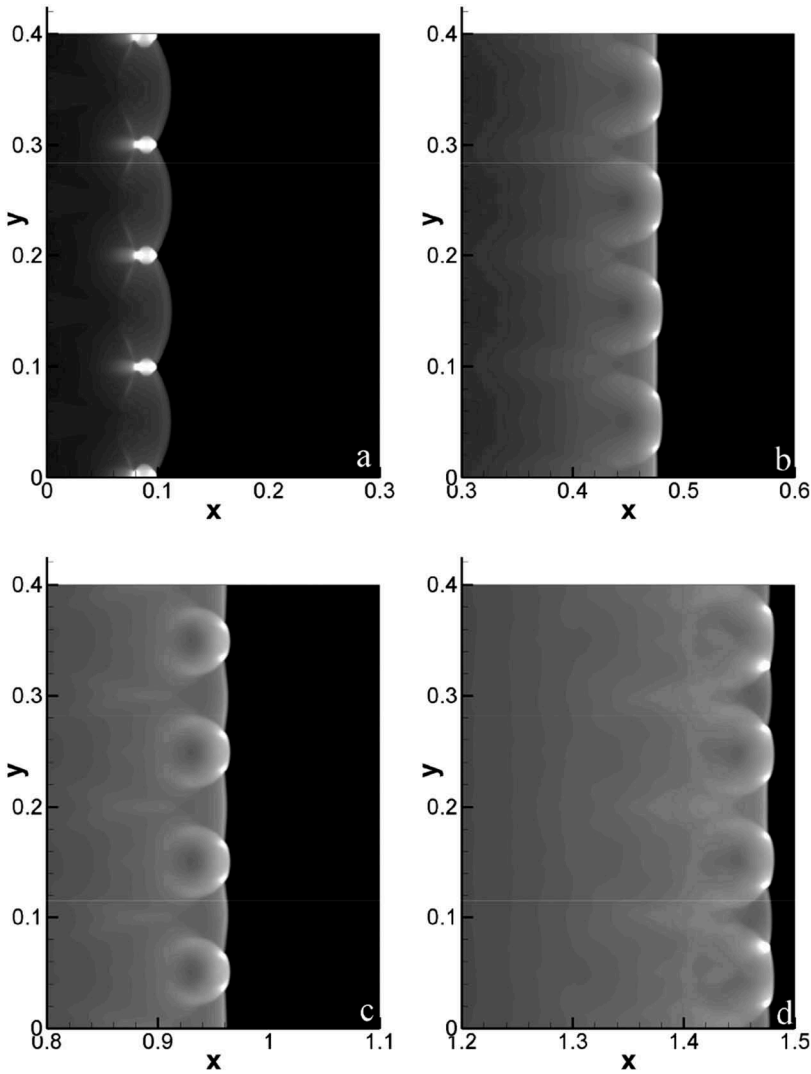


Figure 4. Pressure of cellular detonations based on realistic heat capacity model, $D_p = 4.0 \mu\text{m}$.

transverse waves increases when the constant heat capacity model is adopted, demonstrating the cell width becomes small. Therefore, the cellular structure of 2D detonations is influenced by the realistic heat capacity, and the constant heat capacity model may underestimate the cell width.

The determination of cell width for gaseous detonations is not a trivial task (Sharpe and Radulescu 2011; Taylor, Kessler, Gamezo et al. 2013), but in our case, the cellular structure is very regular and it is easy to count the detonation cells. The lack of reliable experimental data introduces considerable difficulty in calculating particle-air detonations. (Multi-phase detonations must be generated and studied in large-scale facilities, because the cell widths of multi-phase detonations are usually much larger than those of gaseous detonations.) This introduces several problems such as the fuel dispersion, detonation initiation, and flow visualization. Accordingly, previous studies have only confirmed the existence of

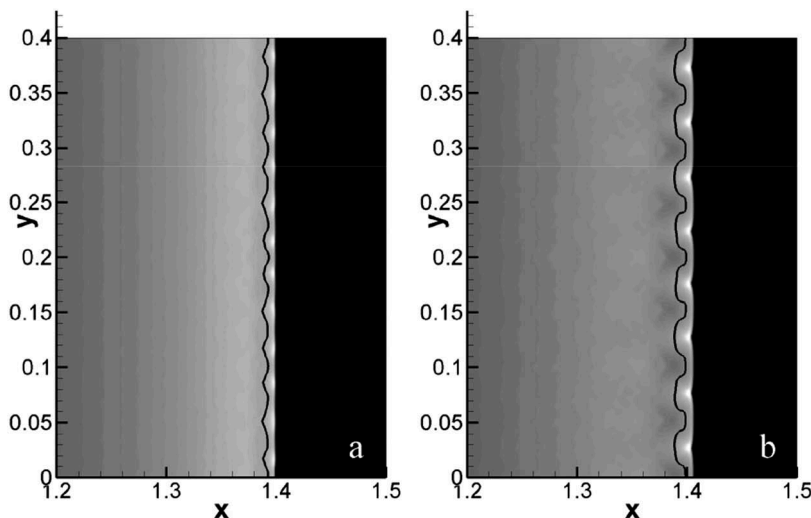


Figure 5. Pressure of cellular detonations based on constant heat capacity model, $D_p = 3.0$ (a) and $4.0 \mu\text{m}$ (b).

transverse waves, but corresponding detonation structures have not been fully elucidated to the best of our knowledge.

Cell width is the most important parameter in gaseous detonations, because it is the basis of several important theories such as the detonation limit, initiation energy, and critical tube diameter (Lee 2008). To model the dusty detonation more efficiently from the quantitative point of view, we averaged in the transverse direction the flow profiles of several cellular 2D detonations to obtain mean 1D longitudinal profiles for the mean pressure and temperature. Similar analysis has been performed for gaseous detonations (with Favre averages) to study the interior hydrodynamic length (Radulescu, Sharpe, Law 2007). Figure 6 shows the averaged pressure, gas temperature, and particle temperature with $D_p = 3.0 \mu\text{m}$. The plateau on the particle temperature is derived from the latent heat of Al (Teng and Jiang 2013). Between two cases, the realistic heat capacity decreased the pressure and temperature and slowed the relaxation of gas and particle temperatures.

The averaged detonation profiles with $D_p = 4.0 \mu\text{m}$ are shown in Figure 7. The profile of the constant case (Figure 7b) was close to those with $D_p = 3.0 \mu\text{m}$, with some corresponding positions (such as decreased overshoot of pressure and particle temperature plateau) did form. This was derived from the slow combustion due to the large diameter, which we also observed in a 1D scenario. However, the profiles were different in the case of $D_p = 4.0 \mu\text{m}$ with the realistic heat capacity model. The shock diffused severely and the particle temperature plateau disappeared, as shown in Figure 6a. As evidenced by the flow field, strong transverse waves formed and the leading shock was intensely curved; to this effect, diffusion structures formed when the detonation was averaged into quasi-1D.

In our previous study, the characteristic length is defined by starting from the leading shock and ending at Al boiling temperature 2792 K, roughly representing the combustion lengths. In this paper, another two characteristic lengths are added in Table 1. The first characteristic length is the full length of the complete particle combustion zone. As the equivalent ratio of aluminum particle to air mixture is about 1.6, and the aluminum

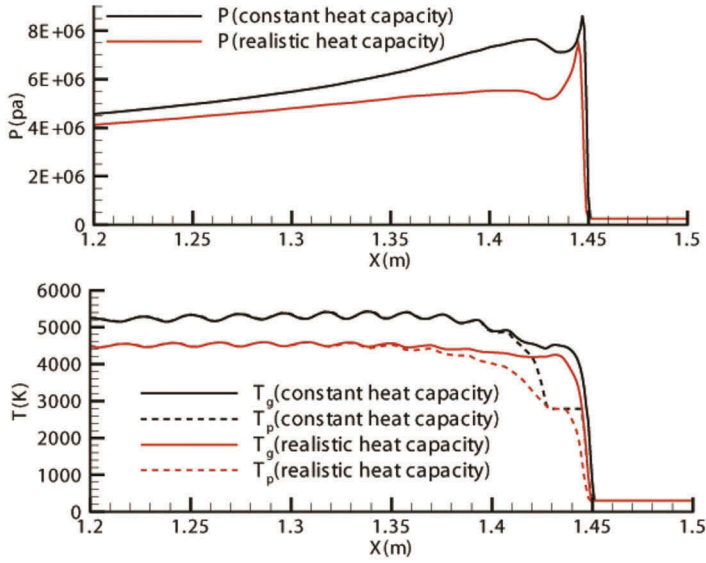


Figure 6. Averaged pressure and temperature of cellular detonations based on the realistic and constant heat capacity model, $D_p = 3.0 \mu\text{m}$.

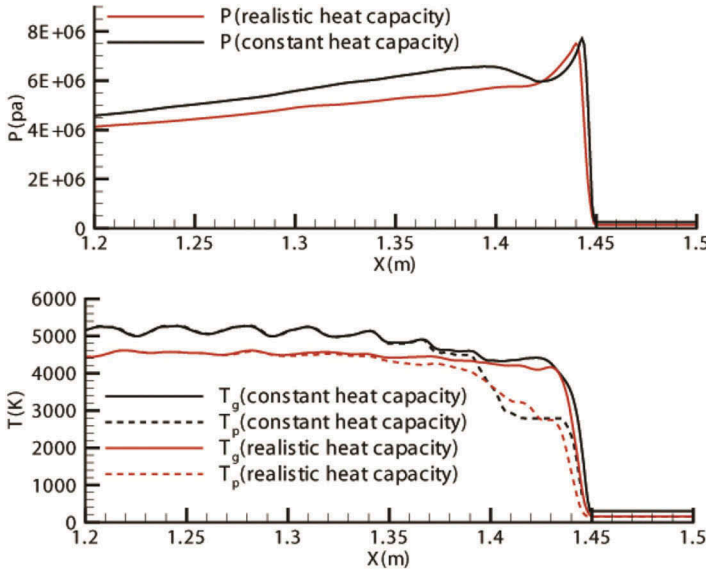


Figure 7. Averaged pressure and temperature of cellular detonations based on realistic and constant heat capacity models, $D_p = 4.0 \mu\text{m}$.

particle is excessive, the full length of the combustion zone can be determined by the total consumption of oxygen in the air, which is defined by starting from the leading shock and ending at the total consumption of oxygen (Table 1). The second characteristic length is the length of the zone from the shock front to the CJ point where $(D-u)/c =$

Table 1. Characteristic length of Al particle-air detonations.

D_p	1D cases		Quasi-1D cases(Al boiling temperature)	
	constant	realistic	constant	realistic
3 μm	6 mm	12 mm	9 mm	15 mm
4 μm	10 mm	19 mm	14 mm	23 mm
D_p	Quasi-1D cases(Full length)		Quasi-1D cases(CJ point)	
	constant	realistic	constant	realistic
3 μm	11mm	15 mm	10 mm	16 mm
4 μm	18 mm	21 mm	15 mm	22 mm

1, the location of CJ point is also given in Table 1. In the case of Figures 6 and 7b, the end corresponds to the front tip of the particle temperature plateau, which is found to be a proper parameter to model the combustion features. Table 1 lists the characteristic lengths of cases $D_p = 3.0 \mu\text{m}$ and $D_p = 4.0 \mu\text{m}$. Both the effect of particle diameter and realistic heat capacities were the same in quasi-1D cases compared to real 1D cases, however, quasi-1D cases have large length scale, so the transverse waves diffused throughout the whole detonation. Gaseous detonation shares this feature (Lee 2008), suggesting that transverse waves play similar roles in detonation propagation in both gaseous and dusty detonations.

It is interesting to note that the case of $D_p = 4.0 \mu\text{m}$ with constant heat capacity has almost the same characteristic length as the case of $D_p = 3.0 \mu\text{m}$ with realistic heat capacity, and both cases manifest four pairs of transverse waves. Due to the so-called mode locking (Sharpe and Radulescu 2011; Zhang et al. 2014), the determination of the exact cell width is difficult, and in some cases the cell width is not a value but a spectrum (Zhang and Bai 2014; Zhang et al. 2016). Barthel (Barthel, 1974) proposed the method to predict the cell width. Further improvements were done by Fedorov & Khmel (Fedorov 2005) for the cellular heterogeneous detonation of aluminum particles in oxygen.

Another characteristic parameter is the detonation velocity, which is about 1470m/s for $D_p = 2.0 \mu\text{m}$ case in the experiment and the peak pressure is 26.0–28.4 times higher than the initial pressure. In the 1D simulations, the corresponding velocity is about 1830 m/s based on the constant heat capacity model, while is about 1630m/s based on the realistic heat capacity model. In the 2D simulations, the corresponding velocities are close to those from 1D simulations, e.g. about 1625 m/s based on the realistic heat capacity model. Furthermore, both 1D and 2D detonations have a peak pressure of 32.2 times with the realistic heat capacities. However, the velocities decrease when D_p increases in the 2D simulations. For example, in D_p 4.0 μm cases, the velocity based on the realistic heat capacity model is about 1542 m/s, and the velocity based on the constant heat capacity model is about 1702 m/s, about 100 m/s decrease for both cases. This is different from 1D simulation, in which the velocities are almost independent on the particle diameters. The velocity-diameter independence demonstrates that with this combustion model, the pre-CJ plane heat release is almost the same regardless the particle diameter. Nevertheless, the inclusion of transverse waves changes the heat release process, inducing the velocity decrease in the large particle cases. The difference of 1D and 2D detonation velocity becomes significant in the large cell width, and vice versa.

Conclusions

Two-dimensional cellular Al particle-air detonations are simulated in this study and the realistic heat capacity effects are analyzed and discussed above. The particle diameter influences cell width, which increases with diameter. This characterization is not only suitable for the realistic heat capacity model, but also the constant heat capacity model. By comparing the results based on realistic and constant models, we found that the cell width is underestimated without realistic heat capacities. A similar conclusion on the combustion characteristic length of 1D detonation is reached in a previous study. To build the connection of the cell width and combustion length, we average the 2D cellular detonations to quasi-1D, demonstrating that the length scale of quasi-1D detonation is larger than that of the truly 1D model. Furthermore, the velocity of 2D cellular detonation is found to decrease when increasing the particle diameter, different from the 1D cases, and the velocity difference becomes significant for large particles.

Due to lack of reliable experimental results, these results cannot be directly validated through experimentation. We should mention that we did not intend to build a model capable of simulating cell width with complete accuracy. Relatively little is known about post-shock multi-phase combustion in terms of numerical cell width. For example, Borisov et al. (Borisov et al. 1991) noted that aluminum oxide does not exist at temperatures above the boiling temperature, which means the complicated chemical kinetics needs to be included to mend the over-high temperature in the current model. There is still much work to be done to build a more mature particle-air detonation model which utilizes realistic heat capacities.

Funding

This work was supported by the National Natural Science Foundation of China [Grant No. 11822202 and 91641130], the Fundamental Research Funds for the Central Universities of China [Grant No. 31020170QD087] and the Basic Research Plan of Natural Science in Shaanxi Province—General Project (Youth) [2019]JQ-132].

References

- A J, T., and J. R. Selman. 1982. Detonation tube studies of aluminum particles dispersed in air. *Symp. Combust.* 19 (1):655–63. Elsevier. doi:10.1016/S0082-0784(82)80240-3.
- Barthel, H. O. 1974. Predicted spacings in hydrogen-oxygen-argon detonations. *Phys. Fluids* 17 (8):1547–53. doi:10.1063/1.1694932.
- Bartlett R W, Ong J N, Fassell W M, Papp C A. 1963. Estimating aluminium particle combustion kinetics. *Combust. Flame* 7:227–34. doi:10.1016/0010-2180(63)90187-1.
- Bazyn, T., H. Krier, and N. Glumac. 2006. Combustion of nanoaluminum at elevated pressure and temperature behind reflected shock waves. *Combust. Flame* 145 (4):703–13. doi:10.1016/j.combustflame.2005.12.017.
- Benkiewicz, K., and K. Hayashi. 2003. Two-dimensional numerical simulations of multi-headed detonations in oxygen-aluminum mixtures using an adaptive mesh refinement. *Shock Waves* 12 (5):385–402. doi:10.1007/s00193-002-0169-7.
- Benkiewicz, K., and K. A. Hayashi. 2006. Parametric studies of an aluminum combustion model for simulations of detonation waves. *Aiaa J.* 44 (3):608–19. doi:10.2514/1.20412.
- Borisov, A., B. A. Khasainov, B. Veyssiere, E. L. Saneev, I. B. Fomin, and S. V. Khomik. 1991. Detonation of aluminum suspensions in air and oxygen. *Khimicheskaya Fizika* 10 (2):250–72.

- Borisov A A, Khasainov B A, Saneev E L, Fomin I B, Khomik S V, Veyssiere B. 1991. *On the detonation of aluminum suspensions in air and in oxygen[M]//Dynamic structure of detonation in gaseous and dispersed media*. Netherlands: Springer. 215–253.
- Briand, A., B. Veyssiere, and B. A. Khasainov. 2010. Modelling of detonation cellular structure in aluminium suspensions. *Shock Waves* 20 (6):521–29. doi:10.1007/s00193-010-0288-5.
- Brooks, K. P., and M. W. Beckstead. 1995. Dynamics of aluminum combustion. *J. Propul. Power* 11 (4):769–80. doi:10.2514/3.23902.
- Dreizin, E. L. 2000. Phase changes in metal combustion. *Prog. Energy Combust. Sci* 26 (1):57–78. doi:10.1016/S0360-1285(99)00010-6.
- Eckhoff, R. K. 1993. Dust explosion research. State-of-the-art and outstanding problems. *J. Hazard. Mater.* 35 (1):103–17. doi:10.1016/0304-3894(93)85026-B.
- Fedorov, A. V. 2005. Numerical simulation of formation of cellular heterogeneous detonation of aluminum particles in oxygen. *Combust. Explos. Shock Waves* 41 (4):435–48. doi:10.1007/s10573-005-0054-7.
- Fedorov, A. V., and V. M. Fomin. 1999. Non-equilibrium model of steady detonations in aluminum particles-oxygen suspensions. *Shock Waves* 9 (5):313–18. doi:10.1007/s001930050191.
- Fedorov, A. V., V. M. Fomin, and T. A. Khmel'. 2009. Mathematical modeling of heterogeneous detonation in gas suspensions of aluminum and coal-dust particles. *Combust. Explos. Shock Waves* 45 (4):495–505. doi:10.1007/s10573-009-0060-2.
- Fedorov, A. V., and T. A. Khmel. 2012. Characteristics and criteria of ignition of suspensions of aluminum particles in detonation processes. *Combust. Explos. Shock Waves* 48 (2):191–202. doi:10.1134/S0010508212020086.
- Fedorov, A. V., T. A. Khmel, and Y. V. Kratova. 2008. Shock and detonation wave diffraction at a sudden expansion in gas-Particle mixtures. *Shock Waves* 18 (4):281–90. doi:10.1007/s00193-008-0162-x.
- Fedorov, A. V., T. A. Khmel, and Y. V. Kratova. 2010. Cellular detonation diffraction in gas-Particle mixtures. *Shock Waves* 20 (6):509–19. doi:10.1007/s00193-010-0290-y.
- Glassman, I., R. A. Yetter, and N. G. Glumac. 2014. *Combustion*. Academic press, New York, USA.
- Hu, Z. M., H. S. Dou, and B. C. Khoo. 2011. On the modified dispersion-controlled dissipative (DCD) scheme for computation of flow supercavitation. *Comput Fluids* 40 (1):315–23. doi:10.1016/j.compfluid.2010.10.001.
- Hu, Z. M., C. Wang, Z. L. Jiang, and B. C. Khoo. 2015. On the numerical technique for the simulation of hypervelocity test flows. *Comput. Fluids* 106:12–18. doi:10.1016/j.compfluid.2014.09.039.
- Lee, J. H. S. 2008. *The detonation phenomenon*. Cambridge university press, Cambridge, UK.
- Linstrom, P. J. 2001. *NIST chemistry webbook*. Gaithersburg, MD: National Institute of Standards and Technology.
- Liu, Q., X. Li, and C. Bai. 2009. Deflagration to detonation transition in aluminum dust-Air mixture under weak ignition condition. *Combust. Flame* 156 (4):914–21. doi:10.1016/j.combustflame.2008.10.025.
- Lynch P, Fiore G, Krier H, Glumac N. 2010. Gas-phase reaction in nanoaluminum combustion. *Combust. Sci. Technol.* 182(7):842–57. doi:10.1080/00102200903341561.
- Lynch, P., H. Krier, and N. Glumac. 2009. A correlation for burn time of aluminum particles in the transition regime. *Proc Combust. Inst.* 32 (2):1887–93. doi:10.1016/j.proci.2008.06.205.
- McBride, B. J., M. J. Zehe, and S. Gordon. 2002. *NASA Glenn coefficients for calculating thermodynamic properties of individual species*. National Aeronautics and Space Administration, John H. Glenn Research Center at Lewis Field, London, UK.
- Melcher, J. C., H. Krier, and R. L. Burton. 2002. Burning aluminum particles inside a laboratory-scale solid rocket motor. *J. Propul. Power* 18 (3):631–40. doi:10.2514/2.5977.
- Oran E S, Weber J W, Stefaniv E I, Lefebvre M H, Anderson J D. 1998. A numerical study of a two-dimensional H₂-O₂-Ar detonation using a detailed chemical reaction model. *Combust. Flame.* 113(1):147–63. doi:10.1016/S0010-2180(97)00218-6.
- Papalexandris, M. V. 2004a. A two-phase model for compressible granular flows based on the theory of irreversible processes. *J Fluid Mech* 517:103–12. doi:10.1017/S0022112004000874.

- Papalexandris, M. V. 2004b. Numerical simulation of detonations in mixtures of gases and solid particles. *J Fluid Mech* 507:95–142. doi:10.1017/S0022112004008894.
- Papalexandris, M. V. 2005. Influence of inert particles on the propagation of multidimensional detonation waves. *Combust. Flame* 141 (3):216–28. doi:10.1016/j.combustflame.2004.12.017.
- Radulescu, M. I., G. J. Sharpe, and C. K. Law. 2007. Lee J H S. The hydrodynamic structure of unstable cellular detonations. *J. Fluid Mech.* 580:31–81. doi:10.1017/S0022112007005046.
- Sharpe, G. J., and M. I. Radulescu. 2011. Statistical analysis of cellular detonation dynamics from numerical simulations: One-step chemistry. *Combust. Theor. Model.* 15 (5):691–723. doi:10.1080/13647830.2011.558594.
- Tanguay V, Goroshin S, Higgins A J, Zhang F. 2009. Aluminum particle combustion in high-speed detonation products. *Combust. Sci. Technol.* 181(4):670–93. doi:10.1080/00102200802643430.
- Taylor B D, Kessler D A, Gamezo V N, Oran E S. 2013. Numerical simulations of hydrogen detonations with detailed chemical kinetics. *Proc Combust. Inst.* 34(2):2009–16. doi:10.1016/j.proci.2012.05.045.
- Teng, H., and Z. Jiang. 2013. Numerical simulation of one-dimensional aluminum particle-air detonation with realistic heat capacities. *Combust. Flame* 160:463–72. doi:10.1016/j.combustflame.2012.10.018.
- Tsубoi, N., K. Eto, and A. K. Hayashi. 2007. Detailed structure of spinning detonation in a circular tube. *Combust. Flame* 149 (1):144–61. doi:10.1016/j.combustflame.2006.12.004.
- Varsakelis, C., and M. V. Papalexandris. 2011. Low-mach-number asymptotics for two-phase flows of granular materials. *J Fluid Mech* 669:472–97. doi:10.1017/S0022112010005173.
- Veysiere, B., B. A. Khasainov, and A. Briand. 2008. Investigation of detonation initiation in aluminium suspensions. *Shock Waves* 18 (4):307–15. doi:10.1007/s00193-008-0136-z.
- Zhang, B., and C. H. Bai. 2014. Methods to predict the critical energy of direct detonation initiation in gaseous hydrocarbon fuels -An overview. *Fuel* 117:294–308. doi:10.1016/j.fuel.2013.09.042.
- Zhang, B., N. Mehrjoo, N. H D, J. H. Lee, and C. Bai. 2014. On the dynamic detonation parameters in acetylene-oxygen mixtures with varying amount of argon dilution. *Combust. Flame* 161 (5):1390–97. doi:10.1016/j.combustflame.2013.11.016.
- Zhang, B., L. Pang, X. B. Shen, and Y. Gao. 2016. Measurement and prediction of detonation cell size in binary fuel blends of methane/hydrogen mixtures. *Fuel* 172:196–99. doi:10.1016/j.fuel.2016.01.034.
- Zhang, F. 2012. Metalized heterogeneous detonation and dense reactive particle flow. *Shock Compression Condens. Matt. R-2011: Proc. Conf. American Phys. Soc. Topical Group Shock Compression Condens. Matt.* 1426 (1):27–34. AIP Publishing.
- Zhang, F., K. Gerrard, and R. C. Ripley. 2009. Reaction mechanism of aluminum-particle-air detonation. *J. Propul. Power* 25 (4):845–58. doi:10.2514/1.41707.
- Zhang, F., H. Grönig, and V. A. Van de. 2001. DDT and detonation waves in dust-air mixtures. *Shock Waves* 11 (1):53–71. doi:10.1007/PL00004060.
- Zonglin, J. 2004. On dispersion-controlled principles for non-oscillatory shock-capturing schemes. *Acta. Mechanica. Sinica.* 20 (1):1–15. doi:10.1007/BF02493566.